

# LOST IN SECULAR EVOLUTION: THE CASE OF A LOW MASS CLASSICAL BULGE

KANAK SAHA

Inter-University Centre for Astronomy and Astrophysics, Pune-411007, India,  
 e-mail: kanak@iucaa.ernet.in  
*Draft version May 27, 2015*

## ABSTRACT

The existence of a classical bulge in disk galaxies holds important clue to the assembly history of galaxies. Finding observational evidence of very low mass classical bulges particularly in barred galaxies including our Milky Way, is a challenging task as the bar driven secular evolution might bring significant dynamical change to these bulges alongside the stellar disk.

Using high-resolution N-body simulation, we show that if a cool stellar disk is assembled around a non-rotating low-mass classical bulge, the disk rapidly grows a strong bar within a few rotation time scales. Later, the bar driven secular process transform the initial classical bulge into a flattened rotating stellar system whose central part also have grown a bar-like component rotating in sync with the disk bar. During this time, a boxy/peanut (hereafter, B/P) bulge is formed via the buckling instability of the disk bar and the vertical extent of this B/P bulge being slightly higher than that of the classical bulge, it encompasses the whole classical bulge. The resulting composite bulge appears to be both photometrically and kinematically identical to a B/P bulge without any obvious signature of the classical component. Our analysis suggest that many barred galaxies in the local universe might be hiding such low-mass classical bulges. We suggest that stellar population and chemodynamical analysis might be required in establishing the evidence for such low-mass classical bulges.

*Subject headings:* galaxies: bulges – galaxies:kinematics and dynamics – galaxies: structure – galaxies:evolution – galaxies:spiral, galaxies:halos

## 1. INTRODUCTION

Classical bulges are typically thought to have formed as a result of violent mergers (Kauffmann et al. 1993; Baugh et al. 1996; Hopkins et al. 2009) or collapse of primordial gas clouds (Eggen et al. 1962) or coalescence of giant clumps in high-redshift galaxies (Immeli et al. 2004; Elmegreen et al. 2008) or multiple minor mergers (Bournaud et al. 2007; Hopkins et al. 2010). Size and mass of these classical bulges depend on the process that formed these stellar system but perhaps little on the subsequent evolution. Observation suggests that the classical bulges are generally dispersion dominated, spheroidal systems which might remain dynamically unchanged over several billion years. A number of recent studies suggest coexistence of classical bulges and bars in disk galaxies (Gadotti 2009; Erwin et al. 2015). Of particular interest are the low-mass classical bulges in barred galaxies, such as our own Galaxy. N-body modelling of BRAVA stellar kinematics reveals that our Milky Way might harbor a low-mass classical bulge inside it's B/P bulge Shen et al. (2010); Di Matteo et al. (2015). For a current summary of the Milky Way's bulge, the readers are referred to Gerhard (2014). Recent simulation by Saha et al. (2012) showed that such a low-mass classical bulge is significantly modified during the secular evolution along with the cool stellar disk. It remains unclear whether such low-mass classical bulges can reliably be detected in observation.

In the initial phase of galaxy evolution, disk galaxies (at high redshift) go through violent instabilities (Genzel et al 2006) and possibly have formed various non-axisymmetric structures (most prominent of which are bar and spiral arms) which, later, drive the slow

secular evolution of these galaxies. In the secular phase, the most efficient way a disk galaxy evolves is through forming a bar which facilitates the redistribution of energy and angular momentum between the disk, dark matter halo and the preexisting classical bulge (Debattista & Sellwood 2000; Athanassoula 2003; Saha et al. 2012). As the bar becomes stronger, it goes through buckling instability and form boxy/peanut bulges as demonstrated in numerous N-body simulation studies (Combes & Sanders 1981; Pfenniger & Norman 1990; Raha et al. 1991; Martinez-Valpuesta & Shlosman 2004; Saha et al. 2012). More than 40% of all observed bulges are B/P bulges (Lütticke et al. 2000) and their observed properties are nicely summarized in Laurikainen & Salo (2015). The formation of a B/P bulge in the central region is an energetically favorable phenomenon, as the B/P bulge is comparatively more random motion dominated than the initial disk. In essence, secular evolution transforms the central part of a cool stellar disk to one with a comparatively hot centrally concentrated bulge (Kormendy & Kennicutt 2004). When such a process takes place in the presence of an initially non-rotating low-mass classical bulge at the center, the secular process also transforms the low-mass classical bulge to a fast rotating object whose kinematic properties resemble that of a B/P bulge, namely having cylindrical rotation in the inner region (Saha et al. 2012). The final composite bulge is a superposition of the B/P bulge and the transformed classical bulge, both of which are cylindrically rotating. The goal of this paper is to find out whether such a low-mass classical bulge can be unmasked from the composite bulge. We present a systematic morphological and kinematic analysis to extract information about the presence of the classical bulge in

the barred galaxy.

## 2. GALAXY MODEL AND SIMULATION

The initial galaxy model, in equilibrium, consists of an initially axisymmetric exponential disk, a cored dark matter halo and a non-rotating classical bulge. The initial classical bulge (hereafter, ICB) is strongly flattened by the disk gravity. The ICB in this galaxy model has a total mass of  $M_b = 0.06M_d$ ,  $M_d$  being the disk mass, and initial ellipticity in edge-on projection is given by  $\epsilon_b = 0.46$ . The initial stellar disk is cool with Toomre  $Q = 1.4$  at  $R = 2.5R_d$ . Further details on the model is given in Saha et al. (2012).

We scale the model such that  $M_d = 4.58 \times 10^{10} M_\odot$  and  $R_d = 4.0$  kpc. Then the time unit is given by 24.9 Myr. We have used a total of 10 million particles. The softening lengths for the disk, bulge and halo particles used are 12, 5 and 20 pc respectively following the suggestion of McMillan & Dehnen (2007). The simulation is performed using the Gadget code (Springel et al. 2001) with a tolerance parameter  $\theta_{tol} = 0.7$ , integration time step  $\sim 0.4$  Myr. The simulation was evolved for a time period of  $\sim 3.0$  Gyr.

## 3. MORPHOLOGY OF THE COMPOSITE BULGE

The initial axisymmetric stellar disk, being cool, rapidly forms a bar with two-armed spiral as shown in Fig. 1. The spiral produces radial heating (Saha et al. 2010; Sellwood & Carlberg 2014), which eventually destroys itself leaving a strongly barred galaxy at the end of the simulation. The end product resembles a typical barred lenticular galaxy without any spiral arm (Cortesi et al. 2013). In the center of this barred galaxy lies the low-mass classical bulge (see rounder contours at  $t = 0$  in Fig. 1). However, as time progresses, even at the very central region ( $< 0.5R_d$ ) the density contours are no longer rounder but are purely elliptical suggesting non-existence of the classical bulge component. We have checked this further inside  $R < 0.2R_d$  and found similar result. In fact, the face-on surface density maps of the classical bulge stars alone (bottom panel of Fig. 1) show that the inner part of this bulge is actually a bar - together with the disk stars, the central part of the galaxy behaves like a single bar component without any structural signature of the classical bulge. It has been shown previously that such a classical bulge actually absorbs a significant fraction of the disk angular momenta emitted by the bar and is transformed into a rapidly rotating bar-like object (Saha et al. 2012).

In edge-on projection, as shown in Fig. 3, the galaxy model at  $t = 0$  has a classical bulge which extends upto about  $0.5R_d$  in the vertical direction along the minor axis. As the bar undergoes buckling instability, it forms a B/P bulge in the inner part of the disk. The outcome of this physical process is a composite bulge which is a superposition of the preexisting classical bulge and the B/P bulge. Such composite bulges are not uncommon and they are reported in a number of barred galaxies, recently studied by Gadotti (2009); Erwin et al. (2015). The vertical extent of the B/P bulge is about  $0.7R_d$  (see Fig. 3) which completely encompass the flattened classical bulge. In other words, the classical bulge camouflages inside the B/P bulge. This may surprise some readers; a priori it is not clear what would be the vertical extent of a

B/P bulge with a given size and mass of a classical bulge to begin with the initial disk. In any case, the generality remains unclear at the moment, as more such N-body experiments are needed. Obviously, massive and bigger classical bulges can be excluded as those can not remain immersed in the B/P bulge. Note the surface density maps of these composite bulges, shown in Fig. 3, appear identical to a pure B/P bulge with no morphological signature of the low-mass classical bulge. In other words, the present study suggests that a B/P bulge in a galaxy might hide a low-mass classical bulge which carries valuable information on the galaxy formation history.

To confirm, we analyzed the surface density profiles at different epochs during the secular evolution of this galaxy model. Fig. 2 depicts the density profile taken at  $t = 113$ . We have performed 3-component decomposition on this barred galaxy model: an exponential stellar disk, sersic bulge and a sersic bar model Gadotti (2009). Our three component decomposition shows that the central region can be well modelled by a pure sersic bulge with sersic index  $n = 1.8$  without a need for a classical bulge, atleast in photometric sense. The radius at which the bulge and disk densities are equal is given by  $R_{bd} = 0.83R_d$ . It appears that the final barred galaxy contains no observable morphological evidence of a classical bulge in the bulge dominated region ( $R < R_{bd}$ ). In the next section, we analyze the kinematics of this composite bulge.

## 4. KINEMATICS OF THE COMPOSITE BULGE

Classical bulges are kinematically hotter with rotational motion intermediate between the ellipticals and B/P bulges (Kormendy & Illingworth 1982). As per kinematics concerned, B/P bulges are further distinguished from the classical bulges, in that B/P bulges possess cylindrical rotation (Kormendy 1982), but see Williams et al. (2011); Saha & Gerhard (2013) for exceptional cases. The kinematics of B/P structures including various projection effects in simulation of disk galaxies are discussed in depth by Debattista et al. (2005); Iannuzzi & Athanassoula (2015).

Fig. 3 depicts the 2D line-of-sight kinematic map (in edge-on projection) e.g., mean velocity and velocity dispersion, before and after the formation of the B/P bulge in our model galaxy. While creating these maps, we have rotated the bar so that its major axis is aligned with the  $x$ -axis and restricted to one projection only. Clearly, the ICB is non-rotating. Once the B/P bulge is formed and evolved, the final composite bulge (classical + B/P bulge) shows clear cylindrical rotation. In addition to the 2D kinematic map, we check this using long-slit kinematics at three different heights above the disk mid-plane ( $z = 0$ ) taken at three different epochs during the secular evolution, see Fig. 4. It is evident from the figure that the classical bulge has a  $V/\sigma = 0$  at  $t = 0$ . The disk rotation velocity rises outward and the velocity dispersion remains nearly flat in the inner region, as a result the local  $V/\sigma$  rises linearly outward. Note that the local  $V/\sigma$  for the slit-1 ( $z/R_d = 0$ ) goes to zero at  $R = 0$  and this basically probes the differentially rotating stellar disk. At subsequent times, we have calculated the local  $V/\sigma$  at  $R_{bd} = 0.83R_d$  and in all cases, we found  $V/\sigma > 1.0$  suggesting a kinematically cool bulge. At  $t = 54$ , the composite bulge rotates cylindrically. The de-

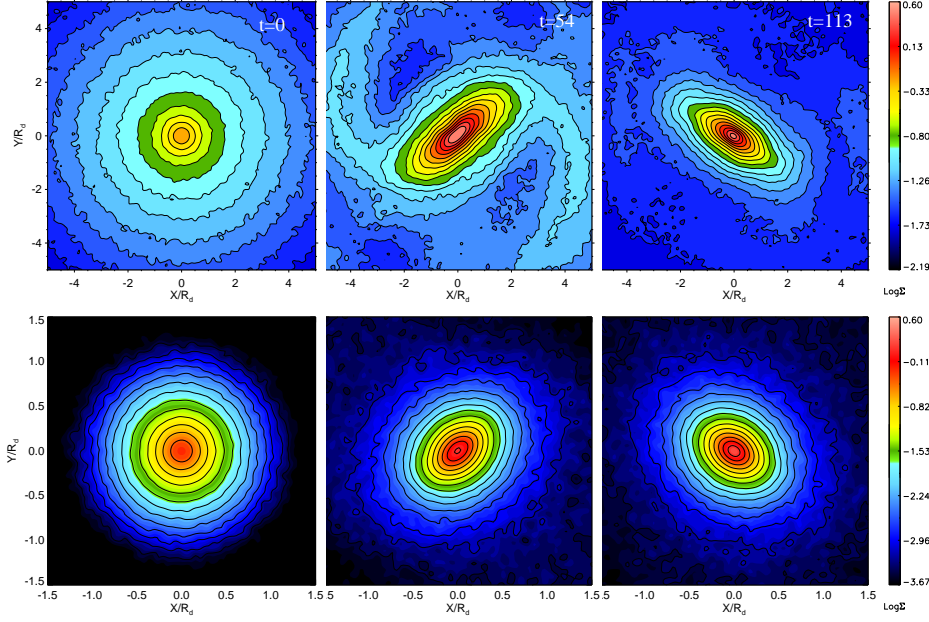


FIG. 1.— Upper panel: face-on stellar surface density (including both disk stars as well as classical bulge stars) maps in model RCG004 at  $t=0$ , 54 and 113 (internal unit). Bottom panel: face-on surface density maps of the classical bulge stars alone at same epochs.

gree of cylindrical rotation becomes stronger with times (as shown by Saha & Gerhard 2013), see the panel at  $t = 113$  of Fig. 4. The major axis velocity dispersion is nearly flat within the extent of the B/P bulge or even within  $R_{bd} = 0.83R_d$  and exhibit a shallow decline beyond that. The local  $V/\sigma$  at  $R_{bd}$  for the composite bulge at  $t = 113$  is close to 1.1 which can be considered as a kinematically cool component (Erwin et al. 2015). But even otherwise, the kinematic signatures are definitely not of a classical component. So far all the kinematic diagnostics suggest that this composite bulge is actually a B/P bulge both morphologically and kinematically. It remains puzzling how to separate classical bulge stars that are hidden inside the B/P bulge.

We then examined the velocity histograms at different locations within the B/P bulge region, more specifically within  $R_{bd} = 0.83R_d$ . First, we looked at the velocity histograms along the minor axis of the bulge as shown in

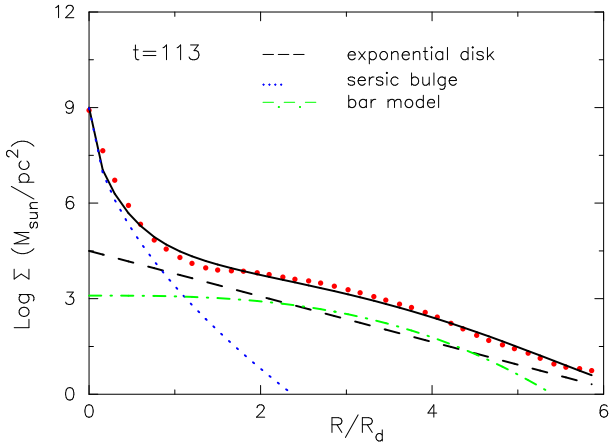


FIG. 2.— Radial surface density profile of the barred galaxy at  $t = 113$  and its decomposition into a bulge+bar+disk. The sersic index of the bulge is  $n = 1.82$  and the bar is modelled with a sersic index  $n = 0.35$ .

Fig. 5 at three different epochs during the secular evolution. Each figure (in both the panels) consists of 3 histograms : for classical bulge stars alone, disk stars alone and the composite bulge (classical + B/P bulge) stars. Note that such an exercise is possible in our N-body simulations as we have a unique ID attached to each particle. As often the case, the bulge, whether classical, B/P or composite bulge, do not show any net rotation about the minor axis. As time progresses, the bar heat up the stars (Saha et al. 2010) as a result of which all the histograms fatten. Interestingly, at  $t = 113$ , all the histograms (due to the classical bulge stars, B/P bulge stars and of the composite bulge) are nearly identical; in other words the minor axis histograms bear no distinguishable sign of the classical bulge. Next we looked at a small area ( $x/R_d = [0.5, 0.6]$ ,  $|y/R_d| = 0.05$ ) along the major axis of the composite bulge - this is depicted in the lower panel of the figure. Initially, the classical bulge stars show no net rotation (histograms in red) and the disk stars show net rotation as per construction of the initial model. At  $t = 54$  and 113, the classical bulge stars show net rotation (see non-zero mean of the velocity histograms) and this nearly coincides with the B/P bulge as well as the composite bulge. Although there is a separate rotating stellar component (here, the classical bulge) sitting inside the B/P bulge, the net velocity histograms of the composite bulge is almost identical to that of the B/P bulge and no detectable signatures of the rotating classical bulge.

At this point, it is useful to recall that the density structures of the classical bulge shows that there is a bar (see Fig. 1 in the central region. This was referred to as the classical bulge-bar, reported in Saha et al. (2012). This classical bulge-bar rotates in sync with the disk bar as can be inferred from position angle of the two of bars at different times during the evolution. As a result of this, there is a fine blend of the classical bulge stars and

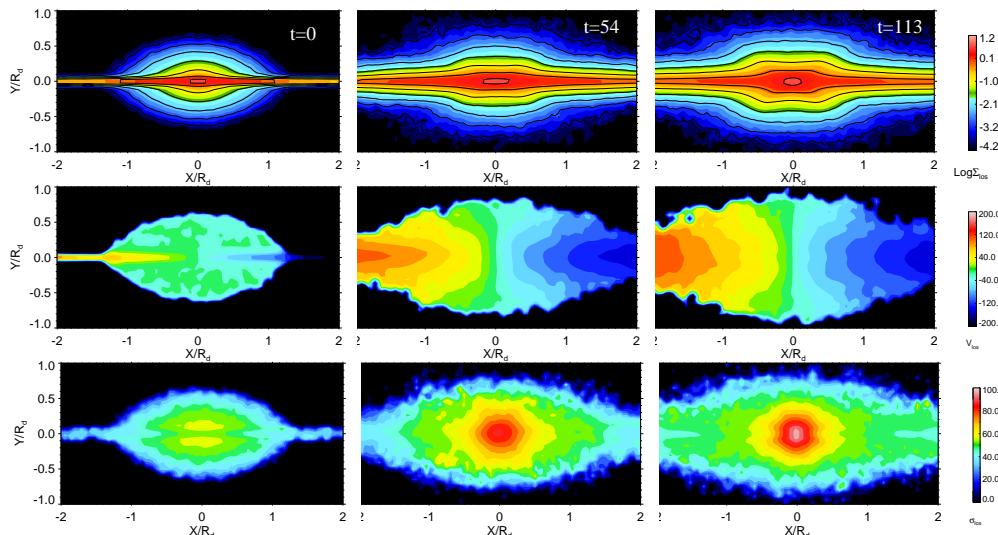


FIG. 3.— 2D line-of-sight moment maps (edge-on projection with the major axis of the bar aligned parallel to x-axis) at three different epochs during the evolution. The upper panel denotes surface density, middle panel the mean velocity and the lower panel the velocity dispersion.

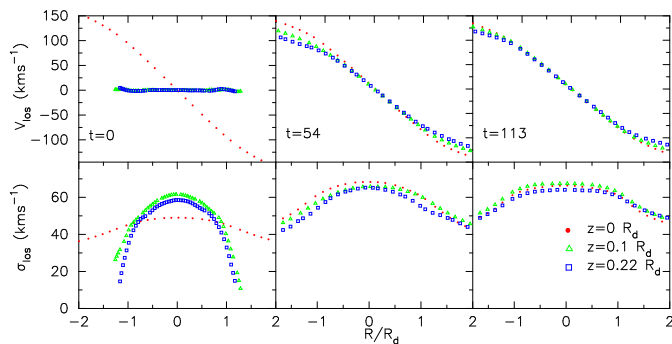


FIG. 4.— Long-slit stellar kinematics from the region covering the composite bulge: the upper panel shows the line-of-sight stellar velocity profiles at 3 different heights above the disk mid-plane during the evolution. The lower panel shows the same but for the velocity dispersion profiles. Note that at  $t = 0$ , the slit at  $z/R_d = 0.1$  and  $0.22$  essentially probe the classical bulge stars.

disk stars that are part of the bar/B/P bulge, explaining the near identicalness of the velocity histograms. In other words, this would explain why the central region, although a composite bulge, behaves both morphologically and kinematically like a B/P bulge with a perfectly hidden low-mass classical bulge.

## 5. DISCUSSION AND CONCLUSIONS

It is generally believed that spheroidal stellar system, of which classical bulges are a subset, do not take part in the secular evolution. Indeed, this may be true if such classical bulges are massive and bigger. But it has been shown by Saha et al. (2012) that very low mass classical bulges get substantially affected by the secular evolution driven by a bar. In fact, what bar driven secular evolution does to a cool stellar disk is to produce a central concentration (Kormendy & Kennicutt 2004), essentially growing a hotter bulge with a  $V/\sigma$  less than that of the disk. Kinematically, a B/P bulge is essentially a vertically thickened bar with hotter stars than what lies beyond the bar's corotation. What secular evolution did to this low mass classical bulge is substantial and quite similar to the disk. The central part of this classical bulge grew a bar (Saha et al. 2012) that is nearly identical to

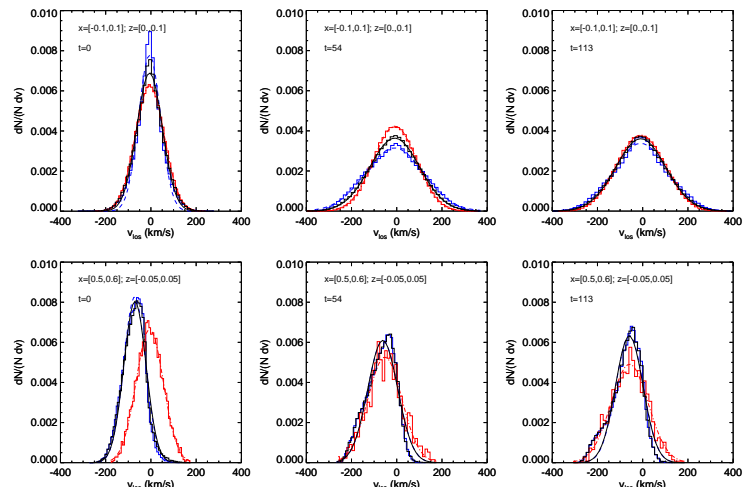


FIG. 5.— Velocity histogram along the minor (upper panels) and major axis (lower panels) of the galaxy model. There is no particular signature of the classical bulge component that resides inside the boxy/peanut bulge. Each histogram is fitted with a Gaussian distribution. Blue and red histograms are due to disk and classical bulge stars alone. The solid black lines represent the histograms of the composite bulge.

the disk bar. The bar later heat the bulge stars as is evident from the minor axis velocity histograms. From this point of view, the classical bulge went through a secular evolution parallel to the disk with similar end products, although not quite the same. The generality of this outcome is not clear at the moment as it requires examining a large number of such high resolution N-body simulations and will be the subject matter of a future paper in the series. In any case, the current analysis produces a twist in a sense that *an apparently pure B/P bulge could actually be a composite bulge with photometrically and kinematically hidden low-mass classical bulge* which could possibly have their origin in mergers/minor mergers (Khochfar & Silk 2006) in accordance with  $\Lambda$ CDM paradigm of galaxy formation.

The next obvious question is whether the presence of these very low mass classical bulges can ever be estab-



lished unambiguously. Observationally, classical bulges tend to show older stellar population, quiescent in star formation activity and populate, in general, the red-sequence of the color-magnitude diagram. In contrast, pseudobulges/B/P bulges exhibit intense star formation and tend to occupy the blue cloud of the color-magnitude diagram. Interestingly, galaxies with comparatively lower mass classical bulges show some amount of star formation activity and about half of these galaxies are barred (Gadotti 2009). In other words, these barred galaxies would be hosting composite bulges with star formation activity intermediate between the pseudobulges and the ones hosting massive classical bulges. If these star formation is driven by minor mergers (Kaviraj 2014; Sachdeva et al. 2015), the preexisting classical bulge would further be contaminated and might increase the level of complexity for the stellar population analysis to draw a firm conclusion on the evidence of a pristine classical bulge. Metallicity gradient could be an im-

portant diagnostic to argue for the evidence of a classical bulge, as it has been done for our Milky Way (Zoccali et al. 2008; Gonzalez et al. 2013; Johnson et al. 2013). Even this can turn out to be a difficult task as the bar would act as a strong agent for mixing and migration (Sellwood & Binney 2002) which would affect the classical bulge stars, might as well erase its imprint. However, if these bulges are formed at the very early epoch of the galaxy assembly history, they might contain extreme metal poor stars like those found in the Milky Way's bulge (García Pérez et al. 2013; Howes et al. 2014) and might convey an important message about the presence of an old classical bulge; of course a number of possibility remains as they could be the halo stars or thick disk stars. In the end, one perhaps has to rely on chemodynamical analysis to obtain a reliable answer.

#### ACKNOWLEDGEMENT

The author thanks the anonymous referee for useful suggestions which improved the manuscript.

#### REFERENCES

- Athanassoula, E. 2003, *MNRAS*, 341, 1179  
 Baugh, C. M., Cole, S., & Frenk, C. S. 1996, *MNRAS*, 283, 1361  
 Bournaud, F., Jog, C. J., & Combes, F. 2007, *A&A*, 476, 1179  
 Combes, F., & Sanders, R. H. 1981, *A&A*, 96, 164  
 Cortesi, A., Merrifield, M. R., Coccato, L., et al. 2013, *MNRAS*, 432, 1010  
 Debattista, V. P., Carollo, C. M., Mayer, L., & Moore, B. 2005, *ApJ*, 628, 678  
 Debattista, V. P., & Sellwood, J. A. 2000, *ApJ*, 543, 704  
 Di Matteo, P., Gómez, A., Haywood, M., et al. 2015, *A&A*, 577, A1  
 Eggen, O. J., Lynden-Bell, D., & Sandage, A. R. 1962, *ApJ*, 136, 748  
 Elmegreen, B. G., Bournaud, F., & Elmegreen, D. M. 2008, *ApJ*, 688, 67  
 Erwin, P., Saglia, R. P., Fabricius, M., et al. 2015, *MNRAS*, 446, 4039  
 Gadotti, D. A. 2009, *MNRAS*, 393, 1531  
 García Pérez, A. E., Cunha, K., Shetrone, M., et al. 2013, *ApJ*, 767, L9  
 Genzel et al. 2006, *Nature*, 442, 786  
 Gerhard, O. 2014, *ArXiv e-prints*  
 Gonzalez, O. A., Rejkuba, M., Zoccali, M., et al. 2013, *A&A*, 552, A110  
 Hopkins, P. F., Cox, T. J., Younger, J. D., & Hernquist, L. 2009, *ApJ*, 691, 1168  
 Hopkins, P. F., Bundy, K., Croton, D., et al. 2010, *ApJ*, 715, 202  
 Howes, L. M., Asplund, M., Casey, A. R., et al. 2014, *MNRAS*, 445, 4241  
 Iannuzzi, F., & Athanassoula, E. 2015, *ArXiv e-prints*  
 Immeli, A., Samland, M., Gerhard, O., & Westera, P. 2004, *A&A*, 413, 547  
 Johnson, C. I., Rich, R. M., Kobayashi, C., et al. 2013, *ApJ*, 765, 157  
 Kauffmann, G., White, S. D. M., & Guiderdoni, B. 1993, *MNRAS*, 264, 201  
 Kaviraj, S. 2014, *MNRAS*, 440, 2944  
 Khochfar, S., & Silk, J. 2006, *MNRAS*, 370, 902  
 Kormendy, J. 1982, *ApJ*, 257, 75  
 Kormendy, J., & Illingworth, G. 1982, *ApJ*, 256, 460  
 Kormendy, J., & Kennicutt, Jr., R. C. 2004, *ARA&A*, 42, 603  
 Laurikainen, E., & Salo, H. 2015, *ArXiv e-prints*  
 Lütticke, R., Dettmar, R.-J., & Pohlen, M. 2000, *A&AS*, 145, 405  
 Martinez-Valpuesta, I., & Shlosman, I. 2004, *ApJ*, 613, L29  
 McMillan, P. J., & Dehnen, W. 2007, *MNRAS*, 378, 541  
 Pfenniger, D., & Norman, C. 1990, *ApJ*, 363, 391  
 Raha, N., Sellwood, J. A., James, R. A., & Kahn, F. D. 1991, *Nature*, 352, 411  
 Sachdeva, S., Gadotti, D. A., Saha, K., & Singh, H. P. 2015, *ArXiv e-prints*  
 Saha, K., & Gerhard, O. 2013, *MNRAS*, 430, 2039  
 Saha, K., Martinez-Valpuesta, I., & Gerhard, O. 2012, *MNRAS*, 421, 333  
 Saha, K., Tseng, Y., & Taam, R. E. 2010, *ApJ*, 721, 1878  
 Sellwood, J. A., & Binney, J. J. 2002, *MNRAS*, 336, 785  
 Sellwood, J. A., & Carlberg, R. G. 2014, *ApJ*, 785, 137  
 Shen, J., Rich, R. M., Kormendy, J., et al. 2010, *ApJ*, 720, L72  
 Springel, V., Yoshida, N., & White, S. D. M. 2001, *NewA*, 6, 79  
 Williams, M. J., Zamojski, M. A., Bureau, M., et al. 2011, *MNRAS*, 414, 2163  
 Zoccali, M., Hill, V., Lecureur, A., et al. 2008, *A&A*, 486, 177